frontiers in Physics

BRIEF RESEARCH REPORT
published: 30 April 2021
doi: 10.3389/fphy.2021.661060

Reconfigurable THz Metamaterial Filter Based on Binary Response for Information Processing System

Eistiak Ahamed[1], *Ahmed Mahfuz Tamim*[1], *Mohammad Rashed Iqbal Faruque*[1]*, *Rasheduzzaman Sifat*[1] *and Mohammad Tariqul Islam*[2]

[1] Space Science Center (ANGKASA), Universiti Kebangsaan Malaysia, Bangi, Malaysia, [2] Department of Electrical, Electronic and Systems Engineering, Universiti Kebangsaan Malaysia, Bangi, Malaysia

Light-matter interactions between the metallic and dielectric layers along with the controlling of electromagnetic waves can create a way to develop micro-devices and moderate the functionalities for advanced applications. This study describes a new controlling technique of the plasmatic electron packet based on an electric split-ring resonator (eSRR). All numerical experiments were performed using an advanced CST electromagnetic package. The proposed metamaterial tunneled structure in this study operates using terahertz (THz) frequency spectrum as an efficient digital processing filter. The array combination of the tunneled structure consisted of three individual unit cells. Moreover, the two engineered metallic arms added to the tunneled structure exhibited two peak resonances and one passband frequency region. A large evanescent field was produced to enhance the wave-metal interactions with the presence of a metal-dielectric micro-tunnel. The intensity of the electromagnetic wave-metal interactions was encoded to binary 0 and 1 for information encoding purposes. As a result, the reconfigurable micro-unit cell metamaterial tunneled structure was able to effectively control the electric field and allow electron packets to be digitally encoded for the information processing system.

Keywords: electric split-ring resonator, digital filter, micro-structured tunnel, reconfigurable, THz

OPEN ACCESS

Edited by:
Weiren Zhu,
Shanghai Jiao Tong University, China

Reviewed by:
Yuancheng Fan,
Northwestern Polytechnical University, China
Jianming Wen,
Kennesaw State University, United States
Xudong Bai,
Shanghai Aerospace Electronics Co., Ltd., China

***Correspondence:**
Mohammad Rashed Iqbal Faruque
rashed@ukm.edu.my

Specialty section:
This article was submitted to Optics and Photonics, a section of the journal Frontiers in Physics

Received: *30 January 2021*
Accepted: *25 March 2021*
Published: *30 April 2021*

Citation:
Ahamed E, Tamim AM, Faruque MRI, Sifat R and Islam MT (2021) Reconfigurable THz Metamaterial Filter Based on Binary Response for Information Processing System. Front. Phys. 9:661060. doi: 10.3389/fphy.2021.661060

INTRODUCTION

Materials with special characteristics like negative permittivity together with negative permeability cannot be found in nature. Thus, engineers or researchers sought to develop artificial materials of different structures exhibiting negative permittivity and negative permeability at a time within a certain frequency spectrum. Such artificial materials are known as metamaterials [1, 2]. One exotic phenomenon of metamaterial is that they can greatly impact the propagation of electromagnetic waves with a superior ability to control the electromagnetic waves as their subwavelength periodic meta-atom unit cell can be designed and optimized for desired applications. In previous works, light-matter interactions in microstructures were optimized to produce non-typical electromagnetic responses. With this in mind, negative electrical permittivity and negative magnetic permeability are included and examined to minimize the gap between basic micro-science and micro-devices [3] alongside the dynamic functionalities of the micro-devices. Metamaterials that can be actively controlled are utilized for numerous applications like controlling the propagation of the electromagnetic wave, analogue computing, [4, 5] etc. Recent studies focus

more on the orbital angular momentum (OAM) of planar metamaterial and metasurfaces [6, 7]. For instance, in an optical transmission system, the OAM of light can be used for multiplexing and to increase the power of the system.

The developmental increase of coded, programmable, and digital metamaterial concepts represent the beginning of a new age in the field of information technology [8–10]. Metamaterials incorporated in digital applications have different exotic characteristics such as beam manipulation [11], broadband diffusion [12], controlling of electromagnetic waves [13], vibration controlling [14], etc. In 2014, Giovampaola and Engheta [15] presented a digital metamaterial concept by constructing metamaterial bytes using spatial mixtures of digital metamaterial bits. The digital metamaterial bits were particles of the materials which indicate explicit material properties of the positive permittivity layer of Silicon (Si) and negative permittivity layer of Silver (Ag). In the following year, a coding metamaterial was developed by Cui et al. [8] for the manipulation of the reflection, scattering, and diffusion of waves in the microwave spectrum. They presented two types of unit cells with 0 and π phases which they named as 0 and 1. They then extended the work from 1-bit coding to 2-bit coding metamaterial. Additionally, Shen et al. [16] presented an integrated Si-based digital metamaterial exhibiting unidirectional energy flow. They also utilized integrated digital metamaterial to develop an optical diode. Furthermore, Shen et al. [17] developed a coding metasurface for beamforming applications based on transmission whereby the transmitted field patterns depended upon the metamaterial bits of the particular meta-atom structure. Meanwhile, Gao et al. [12] presented a coded Minkowski closed-loop structured unit cell to produce several bits on different geometrical scales to control terahertz (THz) radiation.

Moreover, many studies reported numerous micro-electro-mechanical-system (MEMS) based metamaterial and metasurface structures for numerous applications [18–22]. Ma et al. [18] developed polarization-sensitive MEMS-based tunable metamaterials for the terahertz spectrum. The proposed metamaterial structures used curved cantilevers of electric split-ring resonators based on deformable MEMS. In 2014, Han et al. [19] developed a MEMS-based reconfigurable filter and modulator. Low loss and high transparent substrate Quartz was used as a substrate. At 480 GHz, the system manifested a high contrast switching efficiency of 16.5 dB. Meanwhile, Bilgin et al. [20] developed a MEMS-based THz detector which was characterized to extract its mechanical performance in 2015. The detector had a pixel size of 200 × 200 μm, working between 1 and 5 THz bands. Arbabi et al. [21] in 2018, developed a

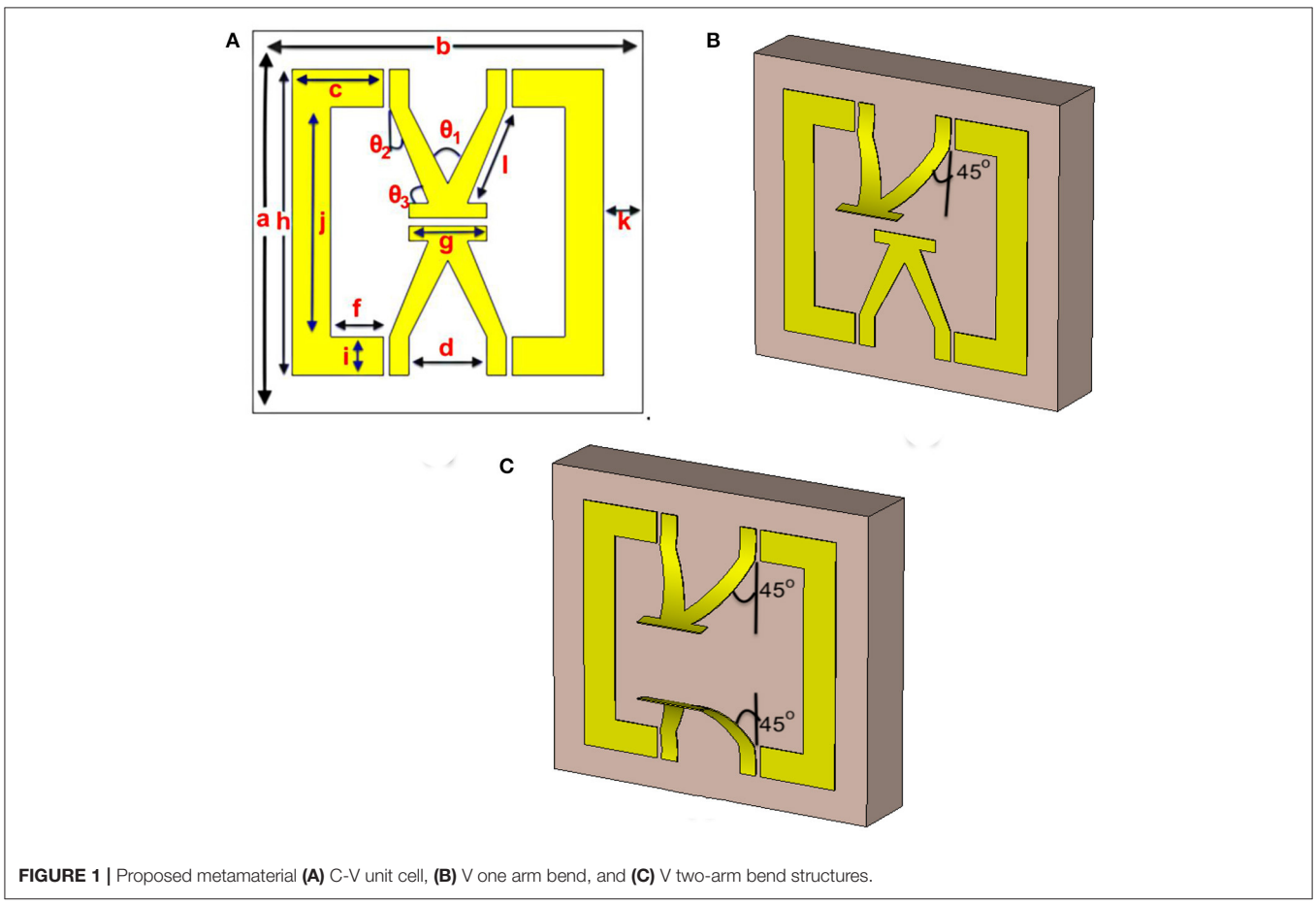

FIGURE 1 | Proposed metamaterial **(A)** C-V unit cell, **(B)** V one arm bend, and **(C)** V two-arm bend structures.

MEMS-based tunable dielectric metasurface lens. The lens was made of MEMS and has an optical power shift of more than 4% per 1 μm movement of the metasurface. In 2020, Huang et al. [22] developed an actively tunable THz filter based on MEMS metamaterial. Due to the advantage in optical applications, electromagnetically induced transparency (EIT) analogues in classical oscillator systems were also discussed. As a functional filter, the metamaterial regulated EIT activity to regulate waves around 1.832 THz.

This study introduces a new reconfigurable metamaterial microstructure that works as a digital filter and is capable of performing bit sequencing conversion in the THz frequency spectrum. The micro-unit cell structure exhibited two transmission resonances and one special passband resonance. A special tunneled arrangement is also presented and numerically explained by digital binary output. Moreover, the basic unit cell is defined as the digital metamaterial by addressing the dielectric substrate as "0" and the metallic resonator as "1." Appropriate tunnel sequencing which was designed and explained can manipulate the electromagnetic waves and convert propagating waves to binary output through a digital metamaterial filter.

TABLE 1 | Geometric parameters of the proposed metamaterial microstructure.

Parameters	Dimensions (μm)	Parameters	Dimensions (μm)
a	10.00	i	1.00
b	10.00	j	6.00
c	2.35	k	2.00
d	2.00	l	2.69
e	0.15	θ_1	45°
f	1.35	θ_2	30°
g	2.00	θ_3	60°
h	8.00		

STRUCTURE OF MICRO METAMATERIAL DEVICE

Figure 1A illustrates the geometry of the metamaterial structure. Its unit cells are composed of corrugated metal strips labeled C to V (C-V) in alphabetical order and periodically arrayed in the x- and y-directions. The C and V strips create horizontal and vertical mirror images, respectively. **Figures 1A–C** present the proposed and modified C-V structures. Whereby, **Figures 1B,C** represent the reconfigurable designs of the C-V structure. which are based on **Figure 1A** [10]. **Figure 1B** displays one arm of V strips that was freed, while **Figure 1C** depicts two arms that were freed from the dielectric interface. On the other hand, lossy metal aluminium utilized in this study possesses an electric conductivity of 3.56 × 10,007 S/m, thermal conductivity of 237 W/k/m and Young's modulus of 69 GPa. The success of aluminium nano-particles in the field of nanoscience and nanotechnology is therefore attributed to their desirable properties. They are non-magnetic, light and non-sparking.

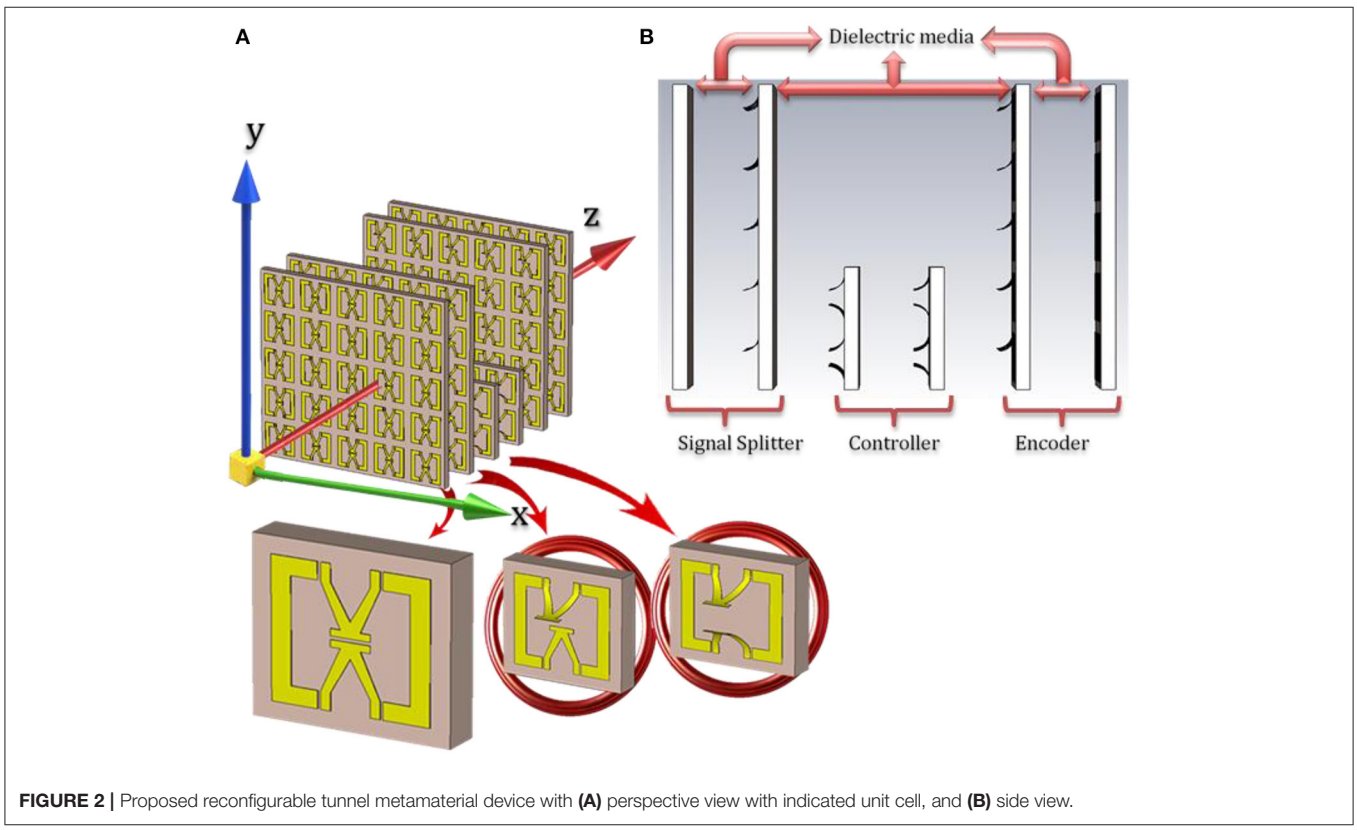

FIGURE 2 | Proposed reconfigurable tunnel metamaterial device with **(A)** perspective view with indicated unit cell, and **(B)** side view.

Also, since they are high in the scale of malleability, they are commonly used in many industrial applications requiring a solid, lightweight and easily constructible material.

Figure 1 and **Table 1** depict the geometrical parameters of the unit cell. The symbols "a" and "b" denote the substrate length and width, respectively. Meanwhile, symbol "e" represents the gap distance between strips C and V, "h" indicates the length of part C, "c" is the width of the two legs in part C, "d" is the gap between the legs of part V, "I" is the metal width of leg C, "j" is the vertical length of strip C, "g" and "l" are the base width and slope of strip V alongside "k" which is the distance between the metal arm and substrate edge. The angles between the two legs of strip V on the bottom inner side, the outer side of the head of strip V, and the bottom outer side of strip V were $\theta_1 = 45^\circ$, $\theta_2 = 30^\circ$, and $\theta_3 = 60^\circ$, respectively. Moreover, the arms of strip V are bent at a 45° angle from the dielectric-metal interface as depicted in **Figures 1B,C**.

Recently, the use of filters in processing optical information has gained the interest of many researchers. Analogous data sets can be encoded for optical communication based on their amplitude, phase, intensity, wavelength, or polarization [23, 24]. Based on these properties, a three-unit cell was designed to create an array to serve as an individual unit cell. The array plates were also used to arrange a parallel sequence to achieve binary information of the proposed micro reconfigurable metamaterial device. Furthermore, the proposed device consisted of four

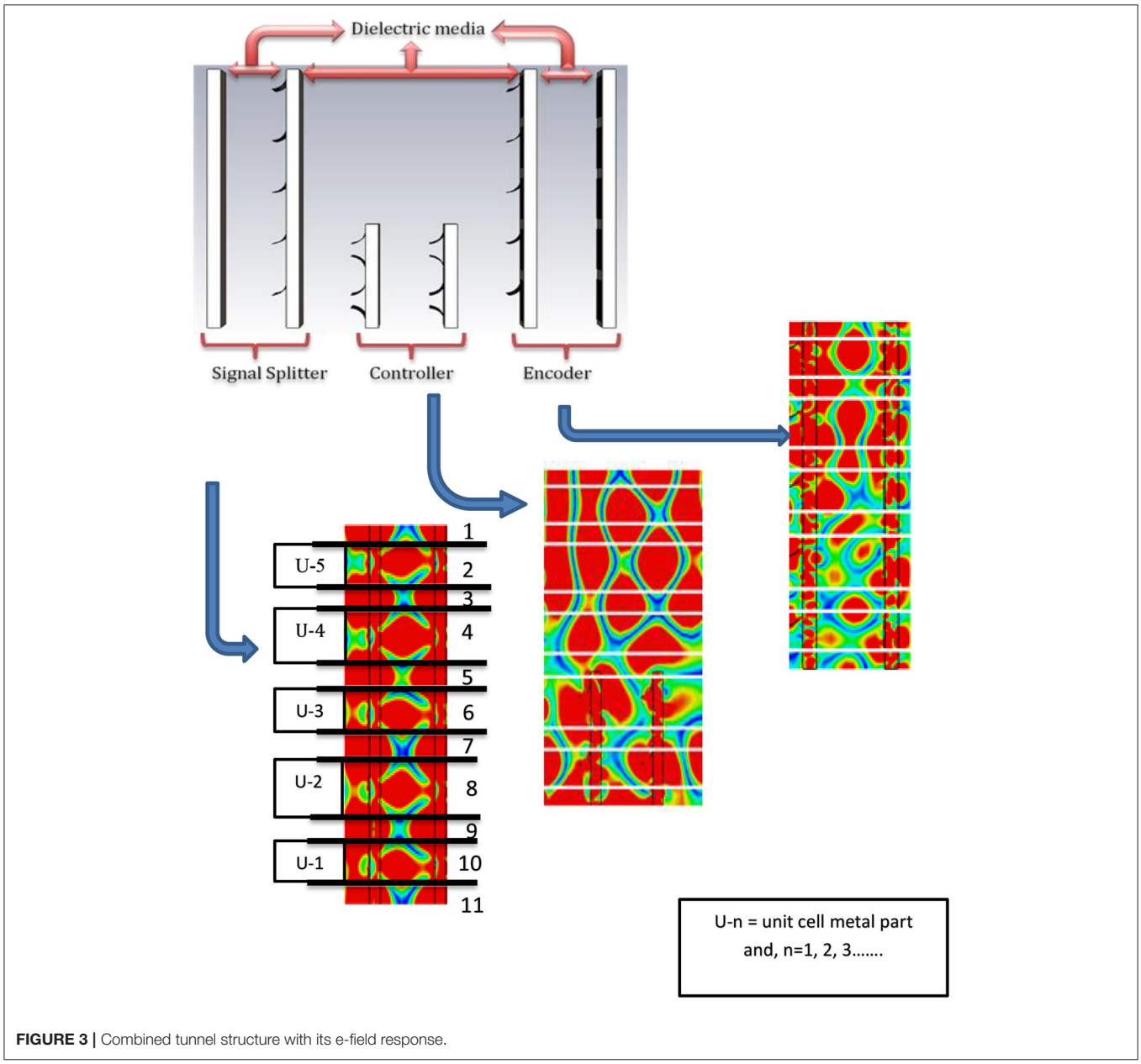

FIGURE 3 | Combined tunnel structure with its e-field response.

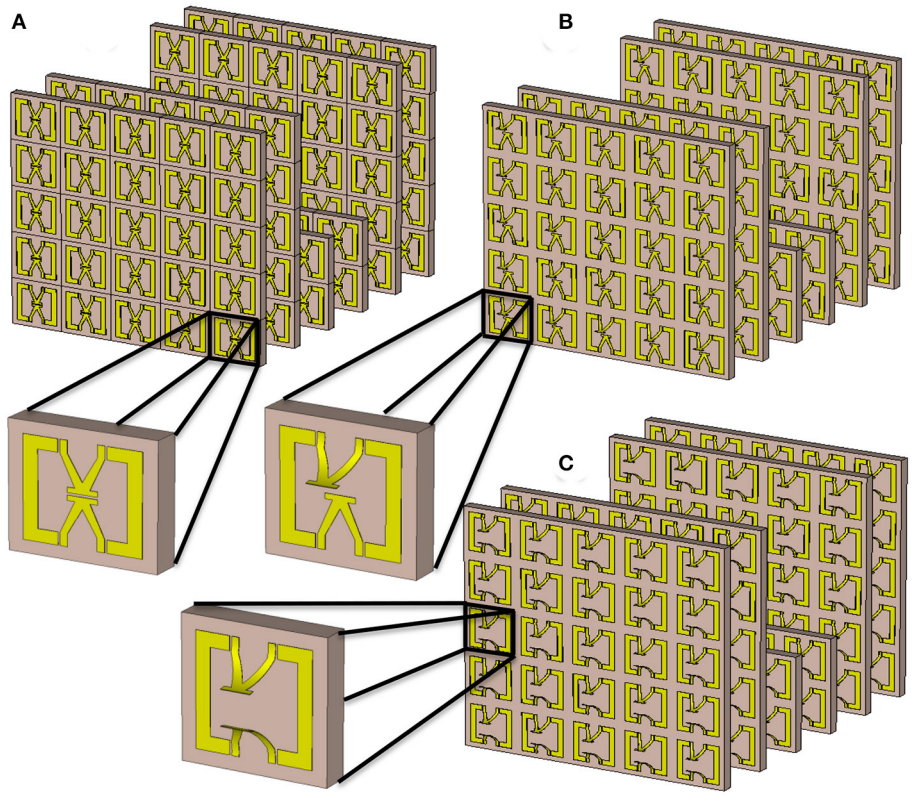

FIGURE 4 | Three different tunnel structures. **(A)** Normal C-V eSRR tunnel structure **(B)** V one arm bend, and **(C)** V two-arm bend of eSRR tunnel structure with unit cells.

different array structures including one arrangement exhibiting tunneling of normal dielectric-metal combination, two providing one- and two-arm bend tunnel combinations and the other exhibiting combined reconfigurable tunnel structure. **Figure 2** indicates the subsequent combinations of the tunnel structure, in which the micro-structured metamaterial tunneled structure was divided into three parts corresponding to the processes of splitting, enhancing, and encoding. According to **Figure 5**, these parts respond to the propagation of electromagnetic waves. The proposed micro metamaterial structure and its operating reconfigurable unit cell are exhibited in **Figure 2**.

The designed C-V metamaterial structure can be modified into a bent structure. After designing three modified reconfigurable structures in one tunnel metamaterial arrangement, the tunnel structure manifested a special response at its passband double negative frequency region. The tunnel structure arrangement is illustrated in **Figure 3**. The first two array structures are of the 5 × 5 array structure indicated by the signal splitter. This part converted the input signal into 11 electron clouds for a 5 × 5 array structure. Following the conversion into 11 clouds, the signal passed through a controller part indicated by the two tunnel arrangements. Here the signal experienced a strong evanescent field effect and was significantly modified. Then, the modified controlled signal finally passed through the encoder part to create binary responses according to field intensity. The procedure is presented in **Figure 3**.

Before designing, the reconfigurable array combination three-unit cells (eSRR) are designed. **Figure 4** exhibits the three-unit cell-based meta-tunnel structure device. All the structures contained a 5 × 5 array unit cell in the signal splitter and encoder region. However, the tunnel area used a 2 × 5 array pattern. The stacked tunnel metamaterial device has six metamaterial array plates, whereby the distance between each plate was 10 μm.

RESULTS AND DISCUSSION

Figures 4A–C depict the proposed eSRR design and the two other tunnel structures. **Figure 5A** describes the scattering parameters of the normal C-V structure. The first structure exhibited transmission resonances of 25.70 and 26.71 THz, with a passband frequency of 25.70 THz. The C-V structure with one V arm bend demonstrated transmission resonances of 25.50 and 26.85 THz (**Figure 5B**), whereas the structure with a tunnel and two V arm bends exhibited transmission resonances of 25.22, 25.98, and 28.75 THz (**Figure 5C**). At the same time, the two reconfigurable structures, namely one arm and two-arm bend structures, exhibited passband resonances of 25.90 and 25.22 THz, respectively. Furthermore, the tunnel structure scattering parameters were better compared to the solid unit cell and array. Meanwhile, the reconfigurable combined tunnel structure exhibited a passband resonance of 29.36 THz.

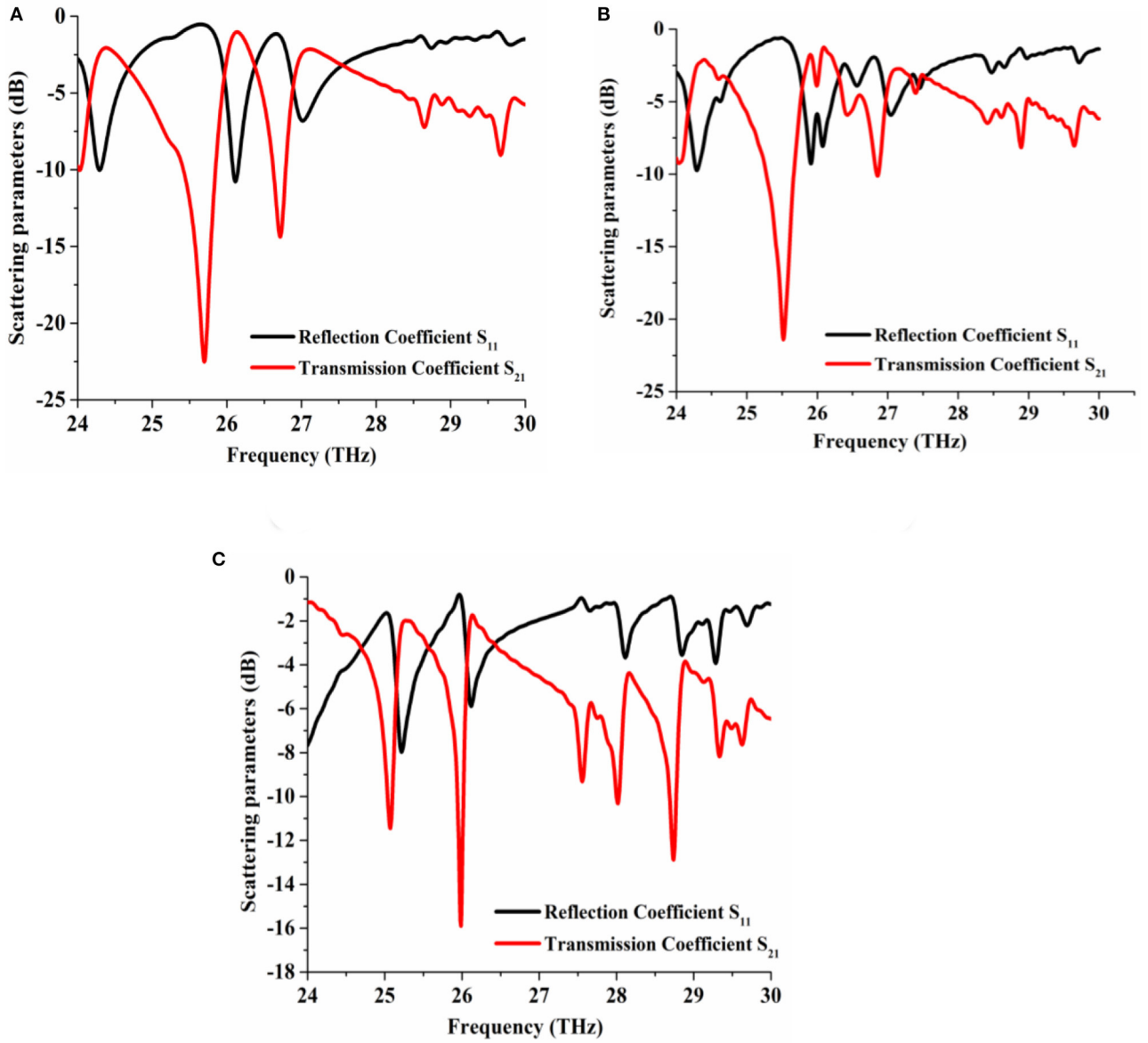

FIGURE 5 | The scattering parameters of **(A)** C-V, **(B)** one arm V-bend, and **(C)** two-arm V-bend proposed structure.

Electrons have a special quality in conveying information from the sender to the receiver. Based on this special behavior, the electric field in a metal-dielectric interface is explored to develop devices like phase shifter, converter, plasmonic power divider, lenses, etc. The evanescent field in the stacked metamaterial tunnel array structure can create different electron cloud patterns that are unavailable in a normal stacked metamaterial array pattern. These metamaterial tunnel array devices could be explained using binary responses. The designed eSRR tunnel structure created a binary response below its $\lambda/2$ limits, while creating a strong evanescent field response in the passband field. The characteristics of the introduced tunnel structures were examined using the transverse electromagnetic (TEM) wave propagation, which interacts partly with the first layer of the metamaterial array and then spreads into eleven clouds of electron regulated by the micro-structured tunnels. The controlled electron clouds were then encoded by the encoding portion whereby the generated signal was delivered to the receiving portion. Next, the modulated electromagnetic electron clouds were transmitted by waveguide port 1 as waveguide port 2 received them. However, based on this condition, the designed four tunnel structures were identified to be in their passband resonances.

In the array pattern, the electric field clouds for the C-V tunnel field contour, V one arm bend, and V two-arm bend in the tunnel field contour are presented in **Figure 6**. The propagation wave

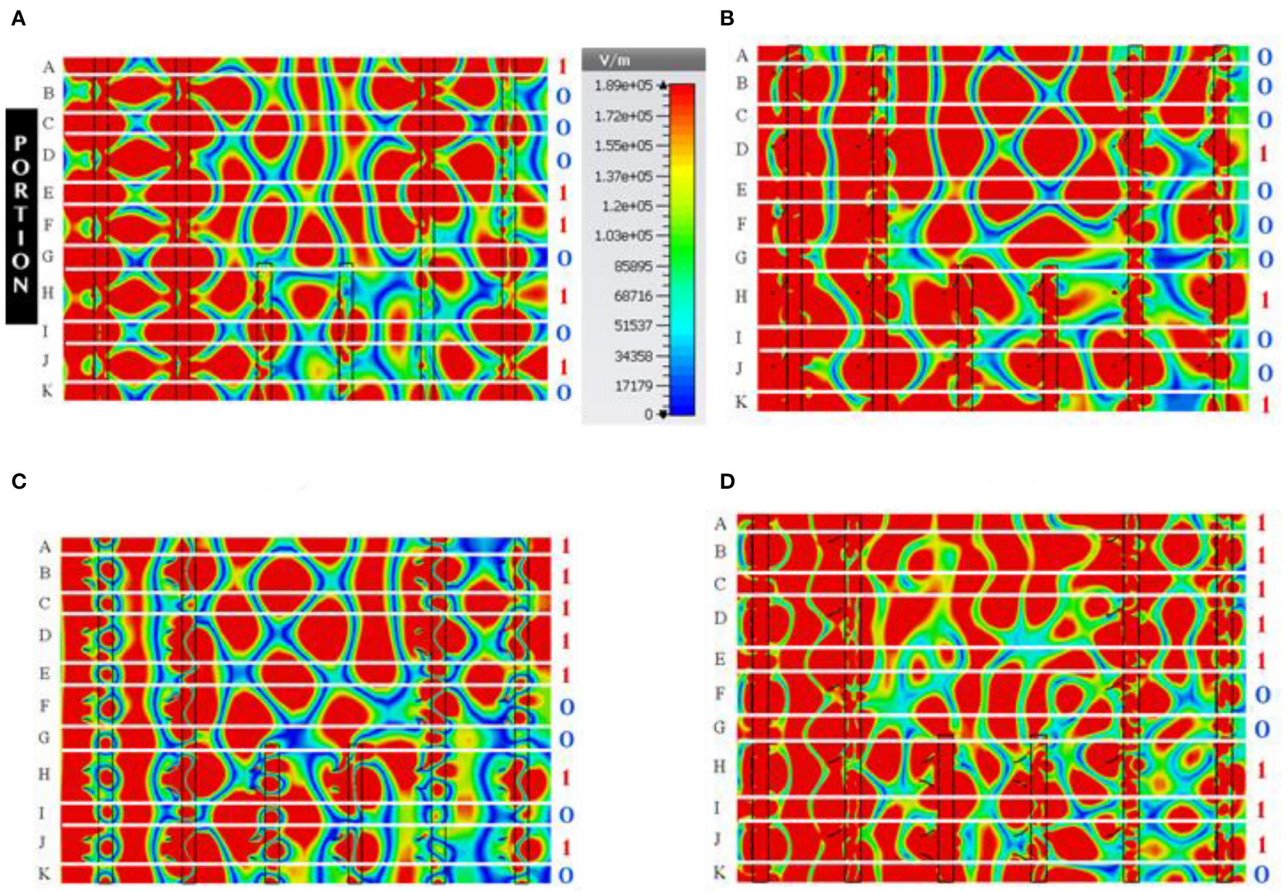

FIGURE 6 | Electric field distributions of the **(A)** C-V tunnel structure, **(B)** One arm V-bend tunnel, **(C)** Two arm V-bend tunnel, and **(D)** Reconfigurable combined C-V tunnel structure.

traveled in a z-direction for all the cases. The tunnel can create a strong evanescent field in a higher frequency region. Therefore, the tunnel array device faces a strong evanescent field contour in the tunnel area. The linear wave experienced a dielectric-metal path in the tunnel area creating a strong evanescent field environment to help obtain different binary responses. In the case of V one arm and two-arm array structures, the wave contours were affected by the dielectric metal interface where its attenuation constant alpha was changed. The wave which experienced a dielectric metal combination with a bend pattern also created a strong evanescent field.

On the other hand, the micro-structured tunnel controlled the strength of the induced electric field. The amplitude of the propagating TEM wave varied when the structural configuration was modified and the electric field intensity was adjusted. When the propagation wave (PW) enters the structure of the first array and gathers information from the last metamaterial slab, the electron clouds formed in the tunnel structure through TEM wave propagation were utilized to convert the electrical signal to information signal as binary output (0 or 1). Therefore, based on the metallic and dielectric parts of the metamaterial tunneled structure, the whole structure can be divided into 11 sections. Firstly, the propagating electromagnetic wave occurred during the first metamaterial collection whereby the modulated electron contour was broken into parts. These contours are

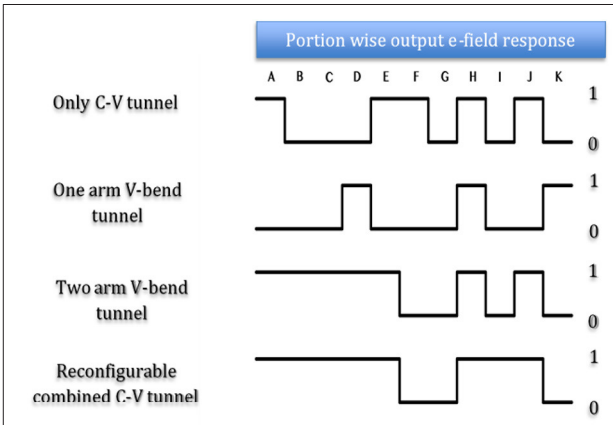

FIGURE 7 | Binary response of the indicated four-tunnel structure.

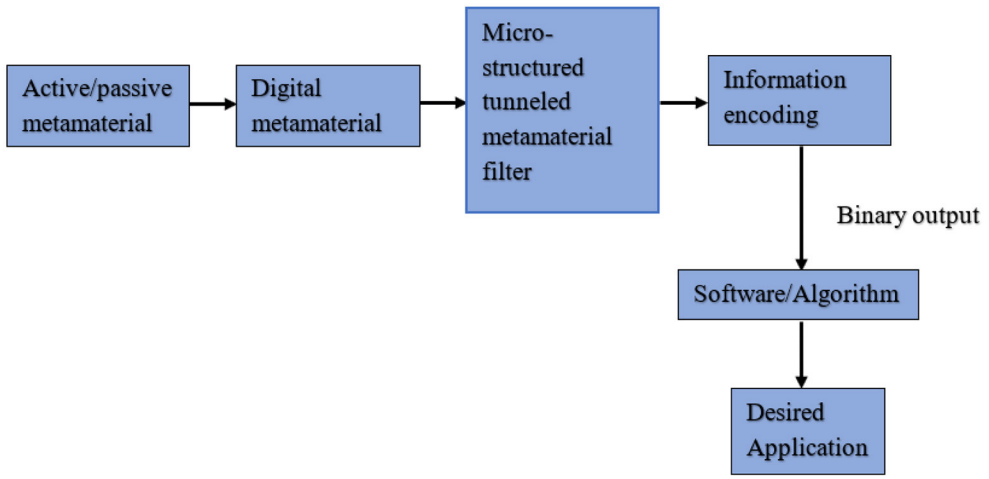

FIGURE 8 | A schematic diagram of the use of digital metamaterial filter for an information processing system.

referred to as a cloud and were transformed when the tunnel was inserted (**Figure 6**) which can be explained digitally. Normally, the movement of free electrons can be used for signal encoding in the forms of current or voltage at the dielectric-metal interface.

The information encoded in this study was digitized based on voltage. Binary output "1" referred to the high voltage red area, whereas the low intensity of the remaining colors was classified as binary "0." Portion A of the passband frequency (25.70 THz) in **Figure 6A** indicated that the electron cloud was digitally high, contributing to a high conversion point. Meanwhile, the converted clouds in portions E, F, H, and J were also digitally high and were represented by "1." However, the digitally low electron clouds in portions B, C, D, G, I, and K were classified as "0." Nevertheless, the tunnel structure response for one V arm bend (**Figure 6B**) was digitally high at portions D, H, and K, while digitally low at portions A, B, C, E, F, G, I, and J with 22.89 THz. High response at portions A, B, C, D, E, H, and J were evident for the two-arm bend V tunnel structure, with low responses at portions F, G I, and J at 22.34 THz (**Figure 6C**). Finally, the combined normal and reconfigurable tunnel structure indicated digital responses at 29.34 THz at which the passband was created. This device exhibited digitally high responses at portions A, B, C, D, E, H, I, and J, whereas digitally low responses were recorded at portions F, G, and K (**Figure 6D**).

The digital responses obtained from various portions of the four-tunnel structure are indicated in **Figure 7**. Electric clouds are dominated by the structure of the tunnel, whereby, all the tunnel arrangements responded differently according to the passband resonances. The e-field responses from **Figure 6A** are summarized in **Figure 7** and indicated by only the C-V tunnel; likewise, three more structures are indicated by its digital responses in **Figure 7**.

A schematic diagram of the information processing system using the micro-structured metamaterial device is illustrated in **Figure 8**. Active or passive metamaterial representing the meta-atom structure generated the meta-atom in a digital form. Next, the micro-structured tunnel configuration was utilized as a filter to encode the binary output from the propagation of waves. Moreover, artificial intelligence (AI) software or algorithm can be used for micro-device applications based on binary outputs.

CONCLUSION

To sum up, a new reconfigurable metamaterial micro-structure was designed and numerically explained based on its binary output to create a digital information filter. The configurations can be completely controlled by the metamaterial tunnel structure arrangement. The electric field was also primarily determined by the configuration of the tunneled micro-structure, whereby the modulated wave signal was encoded to binary output using the proposed meta-device. The entire encoding function was numerically clarified for resonance frequency that corresponded to the reconfigurable tunnel micro-structured metamaterial of one optical passband. A possible schematic diagram of the information processing system was also drawn for the application purpose. In conclusion, the arrangement of the micro-structured tunnel and the flexibility of controlling the moving arms were compatible with an advanced information processing system.

DATA AVAILABILITY STATEMENT

The original contributions presented in the study are included in the article/supplementary material, further inquiries can be directed to the corresponding author/s.

AUTHOR CONTRIBUTIONS

EA and AT: conception and design of the study and analysis of data. EA and RS: initial drafting of the

manuscript. EA, AT, and RS: overall drafting of the manuscript. MF and MI: revising the manuscript critically for important intellectual content. MF: Supervision. All authors contributed to the article and approved the submitted version.

FUNDING

This work was supported by the Research Universiti Grant, Universiti Kebangsaan Malaysia, Dana Impak Perdana (DIP), code: DIP-2020-018.

REFERENCES

1. Smith DR, Pendry JB, Wiltshire MC. Metamaterials and negative refractive index. *Science.* (2004) 305:788–92. doi: 10.1126/science.1096796
2. Siddiky AM, Faruque MR, Islam MT, Abdullah S, Khandaker MU. Inverse double-C shaped square split ring resonator based metamaterial with multi-resonant frequencies for satellite band applications. *Results Phys.* (2020) 19:103454. doi: 10.1016/j.rinp.2020.103427
3. Wang Q, Rogers ETF, Gholipour B, Wang C, Yuan G, et al. Optically reconfigurable metasurfaces and photonic devices based on phase change materials. *Nat Photon.* (2016) 10:60–65. doi: 10.1038/nphoton.2015.247
4. Nan J, Yang R, Xu J, Fu Q, Zhang F, Fan Y. Actively modulated propagation of electromagnetic wave in hybrid metasurfaces containing graphene. *EPJ Appl Metamater.* (2020) 7:9. doi: 10.1051/epjam/2020011
5. Cheng K, Fan Y, Zhang W, Gong Y, Fei S, Li H. Optical realization of wave-based analog computing with metamaterials. *Appl Sci.* (2021) 11:141. doi: 10.3390/app11010141
6. Bai X, Kong F, Qian J, Song Y, He C, Liang X, et al. Polarization-insensitive metasurface lens for efficient generation of convergent OAM beams. *IEEE Antennas Wireless Propag Lett.* (2019) 18:2696–700. doi: 10.1109/LAWP.2019.2949085
7. Li H, Kang L, Dong K. Generating tunable orbital angular momentum radio beams with dual-circular-polarization and dual-mode characteristics. *IEEE Access.* (2020) 8:211248–54. doi: 10.1109/ACCESS.2020.3038568
8. Cui TJ, Qi MQ, Wan X, Zhao J, Cheng Q. Coding metamaterials, digital metamaterials and programmable metamaterials. *Light Sci Appl.* (2014) 3:e218. doi: 10.1038/lsa.2014.99
9. Ma Q, Cui TJ. Information metamaterials: bridging the physical world and digital world. *PhotoniX.* (2020) 1:1–32. doi: 10.1186/s43074-020-00006-w
10. Ahamed E, Faruque MR, Alam MJ, Mansor MF, Islam MT. Digital metamaterial filter for encoding information. *Sci Rep.* (2020) 10:1–9. doi: 10.1038/s41598-020-60170-8
11. Huang C, Sun B, Pan W, Cui J, Wu X, Luo X. Dynamical beam manipulation based on 2-bit digitally-controlled coding metasurface. *Sci Rep.* (2017) 7:1–8. doi: 10.1038/srep42302
12. Gao LH, Cheng Q, Yang J, Ma SJ, Zhao J, Liu S, et al. Broadband diffusion of terahertz waves by multi-bit coding metasurfaces. *Light Sci Appl.* (2015) 4:e324. doi: 10.1038/lsa.2015.97
13. Zhang C, Cao WK, Yang J, Ke JC, Chen MZ, Wu LT, et al. Multiphysical digital coding metamaterials for independent control of broadband electromagnetic and acoustic waves with a large variety of functions. *ACS Appl Mater Interfaces.* (2019) 11:17050–5. doi: 10.1021/acsami.9b02490
14. Liu H, Zhang Q, Zhang K, Hu G, Duan H. Designing 3D digital metamaterial for elastic waves: from elastic wave polarizer to vibration control. *Adv Sci.* (2019) 6:1900401. doi: 10.1002/advs.201900401
15. Giovampaola CD, Engheta N. Digital metamaterials. *Nat Mater.* (2014) 13:1115–21. doi: 10.1038/nmat4082
16. Shen B, Polson R, Menon R. Integrated digital metamaterials enables ultra-compact optical diodes. *Optics Express.* (2015) 23:10847–55. doi: 10.1364/OE.23.010847
17. Shen Z, Jin B, Zhao J, Feng Y, Kang L, Xu W, et al. Design of transmission-type coding metasurface and its application of beam forming. *Appl Phys Lett.* (2016) 109:121103. doi: 10.1063/1.4962947
18. Ma F, Qian Y, Lin YS, Liu H, Zhang X, Liu Z, et al. Polarization-sensitive microelectromechanical systems based tunable terahertz metamaterials using three dimensional electric split-ring resonator arrays. *Appl Phys Lett.* (2013) 102:161912. doi: 10.1063/1.4803048
19. Han Z, Kohno K, Fujita H, Hirakawa K, Toshiyoshi H. MEMS reconfigurable metamaterial for terahertz switchable filter and modulator. *Optics Express.* (2014) 22:21326–39. doi: 10.1364/OE.22.021326
20. Bilgin H, Yalcinkaya AD, Torun H. MEMS-based terahertz detectors. *Proc Eng.* (2015) 120:15–9. doi: 10.1016/j.proeng.2015.08.556
21. Arbabi E, Arbabi A, Kamali SM, Horie Y, Faraji-Dana M, Faraon A. MEMS-tunable dielectric metasurface lens. *Nat Commun.* (2018) 9:1–9. doi: 10.1038/s41467-018-03155-6
22. Huang Y, Nakamura K, Takida Y, Minamide H, Hane K, Kanamori Y. Actively tunable THz filter based on an electromagnetically induced transparency analog hybridized with a MEMS metamaterial. *Sci Rep.* (2020) 10:20807. doi: 10.1038/s41598-020-77922-1
23. Argyris A, Grivas E, Bogris A, Syvridis D. Transmission effects in wavelength division multiplexed chaotic optical communication systems. *J Lightwave Technol.* (2010) 28:3107–14. doi: 10.1109/JLT.2010.2073444
24. Willner AE, Khaleghi S, Chitgarha MR, Yilmaz OF. All-optical signal processing. *J Lightwave Technol.* (2013) 32:660–80. doi: 10.1109/JLT.2013.2287219

Conflict of Interest: The authors declare that the research was conducted in the absence of any commercial or financial relationships that could be construed as a potential conflict of interest.